*Review*

# The Allam Cycle: A Review of Numerical Modeling Approaches

Fabrizio Reale

Institute of Sciences and Technologies for Sustainable Energy and Mobility, STEMS-CNR, 80125 Naples, Italy; fabrizio.reale@cnr.it

**Abstract:** In recent years supercritical $CO_2$ power plants have seen a growing interest in a wide range of applications (e.g., nuclear, waste heat recovery, solar concentrating plants). The Allam Cycle, also known as the Allam-Fetvedt or NET Power cycle, seems to be one of the most interesting direct-fired $sCO_2$ cycles. It is a semi-closed loop, high-pressure, low-pressure ratio, recuperated, direct-fired with oxy-combustion, trans-critical Brayton cycle. Numerical simulations play a key role in the study of this novel cycle. For this reason, the aim of this review is to offer the reader a wide array of modeling solutions, emphasizing the ones most frequently employed and endeavoring to provide guidance on which choices seem to be deemed most appropriate. Furthermore, the review also focuses on the system's performance and on the opportunities related to the integration of the Allam cycle with a series of processes, e.g., cold energy storage, LNG regasification, biomass or coal gasification, and ammonia production.

**Keywords:** allam cycle; $sCO_2$ power cycle; numerical modeling; NET power cycle

## 1. Introduction

The research community has made significant efforts to target the reduction of greenhouse emissions. This involves identifying new thermodynamic cycles, technological solutions or strategies to increase the efficiency of the power plants while decreasing pollutants. An aspect that cannot be overlooked concerns the possibility of continuing to use carbon-based fuels without emitting greenhouse gases.

In this context, the interest in the supercritical $CO_2$ ($sCO_2$) power cycle has exponentially increased in the last years [1], mainly in externally fired applications such as nuclear, waste heat recovery or solar concentrating plants [1–3].

In the last decade, $sCO_2$ gas turbines have been considered also for internal combustion plants: the Allam cycle, also known as Allam-Fetvedt or NET Power cycle, has been conceived by NET Power Inc. within this context. It is a semi-closed loop, high-pressure, low-pressure ratio, recuperated, direct-fired, trans-critical Brayton cycle in which the working fluid is mainly composed of carbon dioxide with fuel and combustion-derived impurities as $H_2O$, inert $N_2$, Ar, and $O_2$. In fact, the heat adduction is guaranteed by an oxy-fuel combustion chamber in which the fuel is burnt with oxygen in an ambient mainly based on carbon dioxide in supercritical conditions.

The 99.5% pure oxygen is provided by a cryogenic air separation unit (ASU) and then introduced with the fuel (e.g., natural gas) within the combustion chamber [4–8].

The ASU is a high energy consumption system; nevertheless, the oxy-fuel combustion maintains similar/higher efficiency levels with respect to air-fired power systems [9].

Figure 1 shows the scheme of the Allam Cycle power plant with auxiliaries, following the scheme analyzed by Scaccabarozzi et al. [10].
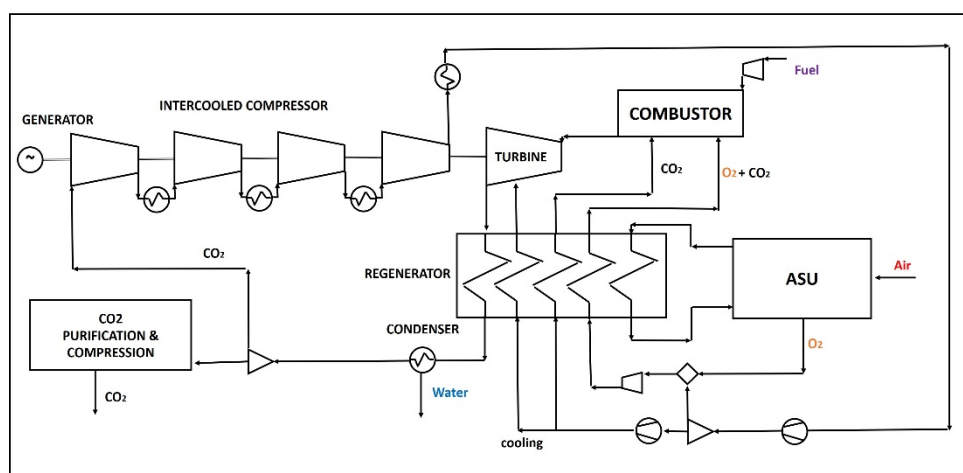
**Figure 1.** Allam Cycle layout.

The carbon dioxide arrives at the intercooled multistage compressor unit and, once in supercritical conditions, to the pump. After pumping, carbon dioxide passes through the regenerator, which is heated by the turbine exhaust heat and the internal low-grade heat from the Air Separation Unit (ASU), in which the oxygen is separated from the air.

A part of $CO_2$ is used for the turbine cooling, while the majority is directed straight into the combustor and a minor mass flow is mixed with the oxygen, coming from the ASU, in all cases after passing within the regenerator. The flow exiting from the combustor is mainly composed of carbon dioxide, water and some impurities. It is expanded in the turbine and comes to the regenerator, heating the above-mentioned fluxes. Then, the exhaust gases, which are at about 30 bar, pass within the condenser to separate the water from the carbon dioxide mass flow and, finally, the excess of $CO_2$ is captured through the purification and compression unit and the main flow, composed of pure $CO_2$, returns to the compressor.

The developers built a 50 MWth test facility in La Porte (Texas, USA) and began testing in 2018. NET Power declares to have accumulated over 1500 h of total facility runs in October 2022. They also projected a utility-scale plant that will be operational within 2026 [11].

Only a few data regarding the demonstration plant are published in the literature. Nomoto et al. [12], Iwai et al. [13] and Suzuki et al. [14] described the demonstration plant combustor and presented their preliminary results. The first tests [12] were carried out at the maximum pressure of 10 MPa, with a lower maximum temperature at the combustor outlet, corresponding to about 55% of full load conditions. The data acquired during the tests highlighted that the combustion efficiency is below 99% at temperatures below 600 °C and approaches 100% at temperatures above 800 °C, considering also that the combustor outlet temperature rises to 850 °C after ignition, while CO concentration at combustor exit is 300 ppmvd or more and unburned $CH_4$ is 25 ppmvd or less.

The tests at different pressures, from 10 to 30 MPa, were described in [13] and the authors underlined that the combustor showed good operability over a wide range of equivalent ratios and $O_2$-$CO_2$ oxidizer percentages.

As concern the turbine, Allam et al. [8] highlighted that the maximum allowable turbine inlet temperature depends on the pressure levels, close to 300 bar, and on the allowable stress level of the nickel alloy; the typical TIT are in the range of 1100–1200 °C.

With these constraints, the turbine has to utilize both gas and steam turbine technologies, as highlighted by Nomoto et al. [12]. The authors focused their attention on the prototype that has been installed within the demonstration plant at La Porte in Texas (US).

Even if the commercial turbine has to operate at 3000–3600 rpm, respectively, at 50 Hz and 60 Hz, the proposed prototype is smaller and faster. The turbine includes seven stages and the paper describes the gas path, cooling and casing design, with a focus on the chosen

materials. In particular, two Ni-based materials defined by Toshiba were chosen for both rotor and casing, while the designed turbine was a double shell structure with both outer and inner casing: the first one was designed using CrMoV casting steel derived from steam turbine technology, while the part of the inner casing that encloses the turbine exhaust was in Ni-based material.

In addition to the aforementioned information, we underline that the concept design of the combustor and turbine of the utility-scale plant could differ from once seen previously. In fact, Toshiba worked with NET Power to develop and design the combustor and turbine of the demonstration plant, while NET Power recently reported that the design and development of the utility-scale combustor and turboexpander will be carried out in cooperation with Baker Hughes [15].

Furthermore, Moore et al. [16] recently developed a 300 MWe utility-scale 6-stage axial turbine layout, focusing the attention also on the cooled blade heat transfer correlations and performing a novel blade optimization.

Despite the lack of experimental data, the growing researchers' interest is simply described by the growing number of scientific articles focused on—or citing—this new cycle. The "Allam cycle" appears in the search results in about 137 documents on the Scopus research engine and in 98 articles in the Clarivate web of science (WoS) research engine as shown in Figure 2 [17,18] (10 September 2023).
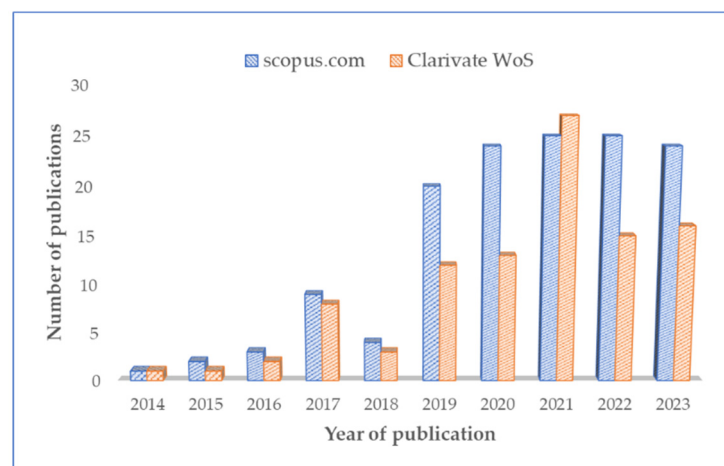


**Figure 2.** Number of publications on the Allam cycle (Scopus vs. wos).

Figure 3 shows the country distribution of the author affiliations from [17]: the authors are mainly affiliated with institutions from the USA, Russia and China.
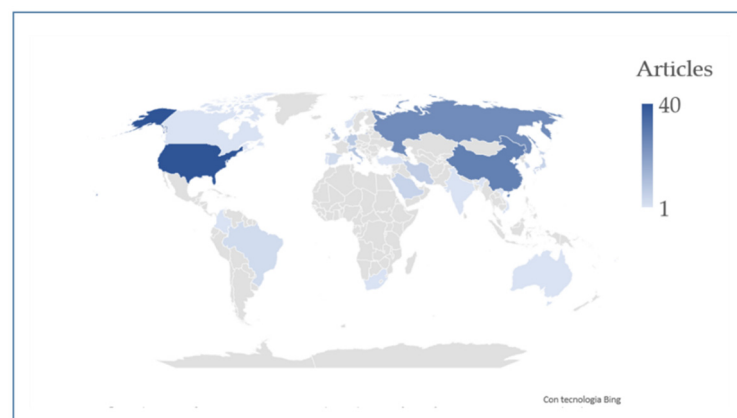


**Figure 3.** Authors' Country affiliation distribution (scopus).

The researchers' interest is addressed in numerical and theoretical studies, partly due to the absence of experimental data and prototypes. Their efforts have mainly centered on the thermodynamic cycle, with attention on energetic, exergetic, techno-economic analysis, and optimization of the cycle.

Several of these studies are also focused on the integration of the Allam cycle in various hybrid systems or on modifications of the cycle, while only a few papers deal with the oxy-fuel combustion process in supercritical carbon dioxide flow.

In this context, the aim of this review is to provide an overview of the modeling approaches used to simulate the Allam cycle, also analyzing the performance of the energy system in order to highlight potentialities and issues. The review is organized as follows: the cycle definition and thermodynamic models have been reviewed in Section 2, both as regards natural gas (Section 2.1) or coal-based fuels (Section 2.2). A comparison of the various models and sub-models is conducted in Section 2.3. Section 3 deals with the numerical simulation in case of modifications and/or integration of the Allam cycle with other components, while Section 4 is focused on the combustion process modeling. Finally, the conclusions of this work are presented in Section 5.

## 2. Cycle Definition and Thermodynamic Models

The Allam cycle is considered one of the most promising power cycles due to its high efficiency, flexibility and economic performance [19].

Table 1 shows the main characteristics of the Allam cycle as described by the developers [4–8].

**Table 1.** Allam Cycle key parameters data.

| Description | Value | Ref. |
|---|---|---|
| Compressor inlet pressure and temperature Turbine inlet pressure | 30 bar, 20 °C | [4] |
| Combustor inlet pressure and temperature | 300 bar, 750 °C | [4] |
| Turbine inlet pressure and temperature | 300 bar, 1150 °C | [4] |
| Natural gas target net efficiency | 58.9% | [5] |
| Coal target net efficiency | 51.44% | [5] |
| Reheated net efficiency | 57.44% | [5] |

The declared net electrical efficiency, as shown in Table 1, is 58.9% for the basic cycle and 57.5% in the case of reheat, in both cases when the fuel is natural gas. In particular, in the case of reheat, the exhaust flow coming from the turbine is used to reheat the recycle stream into the combustor, elevating its temperature [5]. The coal-fired net electrical efficiency is equal to 51.44%.

The results of simulations carried out by several research groups highlighted that these values are usually lower with respect to those reported by the developers.

Regarding this point, Scaccabarozzi et al. [10] assumed that the difference could be related to the consideration or not of the effects of the turbine cooling system on the overall system performance calculations.

In the next subsections, the reviewed numerical studies are presented, reporting the main results, in terms of energetic and exergetic efficiency, both in the case of natural gas (Section 2.1) or coal-based syngas (Section 2.2) fuelling. Section 2.3 summarizes the main characteristics and results of the reviewed articles, highlighting the weight of the modeling choices on the final results. The energetic efficiency is referred to as the fuel LHV, except when differently reported. For each reviewed article, a comprehensive overview of the modeling approach is provided, with a focus on the selected equation of state and the most critical components of numerical constraints. The aim is to provide information that can be valuable for comparing different modeling approaches.

### 2.1. Natural Gas-Based Allam Cycle

Chowdhury et al. [9] conducted a study on the Allam cycle using Aspen HYSYS. The thermodynamic properties have been determined through the Lee-Kesler-Plocker equation of state (EoS) [20,21]. Specific heat during the combustion process was calculated using the NIST database, with the Shomate equation being employed when data were unavailable [22]. The authors conducted also a comparative analysis of the system performance for both liquid and gaseous $CO_2$ recirculation feed scenarios. In the first case, the net plant efficiency is 44.5%, while the latter is 55.1%, for a net power of 262.4 and 324.8 MW, respectively.

Scaccabarozzi et al. [10] built a numerical model of the entire energy system in Aspen Plus v8.4, focusing the attention on the model selection for each component, in order to consider the peculiarities of the carbon dioxide in supercritical conditions. For the expander, they used a modified version of the El-Masri continuous expansion model [23], while for the regenerator, they introduced two multi-flow heat exchangers, considering that multiple pinch points may exist. The selection of the most suitable equation of state has been carried out and the Peng-Robinson equation of state [24] has been identified by the authors as the most suitable to model the cycle. At 100 bar, the specific electric consumption of the ASU is fixed at 1365 kJ/kg$_{O2}$. Results of simulations highlighted that the net electric efficiency of the base case is 54.58%. The authors carried out a sensitivity analysis to various characteristic parameters and a cycle optimization, identifying a net electric efficiency of 54.80% for the maximum efficiency cycle with a considerable difference in the operating conditions. They estimated that the optimal turbine inlet pressure range is between 260 and 300 bar and that the optimal turbine inlet temperature is between 1100 and 1200 °C. They also stated that the cycle efficiency drastically drops below 240 bar.

Hervas et al. [25] carried out a thermodynamic, exergetic and economic analysis of a 300 MWe power plant based on the Allam cycle. The used software is EBSILON Professional 13. The pressure levels are in the range of 30–300 bar, the turbine inlet temperature is equal to 1150 °C and the turbine cooling is also taken into account. The thermodynamic properties of carbon dioxide in supercritical conditions have been considered by selecting the Peng-Robinson equation of state [24]. The ASU and recuperator have been modeled as black-box starting from the data published in [10,26]: the ASU-specific electric consumption is equivalent to 1447 kJ/kg$_{O2}$. Results of simulations highlighted that the net electric efficiency is 53.9%, while the exergetic efficiency is equal to 50.1% and the LCOE is equal to 122 €/MWh.

Penkuhn et al. [27] used Aspen Plus to model the Allam cycle turbine, adopting the Peng-Robinson equation of state for general properties and the Lee-Kesler-Plöcker equation for the carbon dioxide recompression modeling [28]. The turbine inlet pressure and temperature are 300 bar and 1150 °C, respectively. The specific power demand of the ASU is fixed at 900 +/− 150 kJ/kg$_{O2}$ (The authors studied three different cases: a base case, and a low and high-efficiency case. The results of simulations gave a cycle efficiency between 47.9% and 57.2%, with a value for the base case of 53.4%, while the exergetic efficiency was equal to 51.3%. The authors highlighted that the Allam cycle appears to have higher efficiency with respect to other oxy-combustion cycles and that recompression could have a certain potential as an improvement of the cycle.

Colleoni et al. [29] presented the results of thermodynamic analysis of the Allam cycle using Thermoflex v 30.0, a commercial software that incorporates the NIST REFPROP database [30] to account for the thermodynamic properties of $CO_2$ in supercritical conditions. The turbine, designed by Toshiba, has been modeled through seven cooled gas turbine stages. The cooled gas turbine sub-model integrated into Thermoflex is based on El-Masri's GASCAN code [31]. The regenerator has been modeled using three two-stream heat exchangers arranged in series. The modeling approach of the ASU had a resulting specific power consumption of 1326 kJ/kg$_{O2}$. Simulation results showed a net electric efficiency of 49% for the base case, while the efficiency of the optimized case reached 50.4%.

Rogalev et al. [32] developed a construction of a high-power sCO$_2$ gas turbine with optimal thermodynamic parameters of the cycle. The model has been built using Aspen ONE as software, including the model of the air separation unit, determined as the cryogenic high-pressure two-stage. Several approaches have been considered to estimate the CO$_2$ thermodynamic properties: two equations of state (the Peng-Robinson EoS and the Redlich-Kwong EoS) and the NIST REFPROP database. The authors chose to use the NIST-REFPROP database to simulate the Allam cycle because the highest accuracy was highlighted in their comparison with reference data. The open-loop internal cooling of the high-temperature turbine has been considered: the coolant flow fraction has been determined following Wilcock et al. [33] and the cooling losses have been estimated. Results of thermodynamic optimization showed that the highest net efficiency is equal to 56.5% for a turbine inlet temperature and pressure of 1083 °C and 300 bar, a coolant temperature of 200 °C and a turbine outlet pressure of 30 bar. Results of environmental characteristics analysis showed that the specific amount of CO$_2$ emitted to the ambient is 0.0038 kg/kWh, while the total specific investment cost is 1307.5 $/kW. This value is cheaper with respect the costs of CCPP with CCS (2424.3 $/kW).

Chan et al. [34] proposed to introduce the reheating configuration to the Allam Cycle, focusing their attention on the effects of some key parameters on the cycle performance. Simulations were carried out using Aspen Plus v11: the combustor has been simulated through the RGibbs block, the turbine has been modeled using El-Masri's continuous expansion model, while the regenerator consists of two multi-flow heat exchangers connected in series. The optimization has been conducted considering the simulation in Aspen Plus as a black-box function, using the NOMAD algorithm in Matlab, maximizing the net cycle efficiency. Results of simulations and optimization highlighted that the optimization of the base case gives a maximum efficiency of 49.32%, lower than the base case and that the overall power and the specific work are more than two times greater than the original values. The authors also stated that, in the case of a reheated cycle, the heat integration of ASU is not needed, with an increase in the flexibility of the energy system.

Haseli et al. in various studies [35–39] developed and improved a thermodynamic model with the aim to study and optimize the cycle. The author presented an analytical formulation of the Allam cycle performance [35], with a simplified thermodynamic model, which was implemented using Engineering Equation Solver (EES), with several assumptions (e.g., negligible pressure drops, adiabatic behavior of all components, no turbine cooling), applying the p-T relation of ideal gases. In [36] their modeling approach integrated the ASU with the Allam cycle. The ASU power consumption has been fixed at 1354 kJ/kg$_{O2}$. The ASU was described as a double-column distillation consisting of a main air compressor, an air cooler, an adsorption unit, a booster compressor, a main heat exchanger, two air turbines, an oxygen pump and a distillation unit. Results of simplified simulations showed a net cycle efficiency of 54.4% [35], which can be optimized to 59.7% [36]. In the latest study [39] the authors focused their attention also on the importance of estimating the real-fluid properties: the assumption of ideal gas constant properties may lead to a 25–60% overestimation of the power absorbed by the CO$_2$ compressor, while the turbine power prediction can be overestimated by 3–4%. The authors chose to use a correction factor to consider this aspect.

Wimmer et al. [40] compared the Allam Cycle with the Graz cycle. The thermodynamic analysis is conducted using IPSEpro v7 (SIMTECH Simulation Technology, Graz, Austria). The cooled turbine stages are modeled using a previously developed model, while the recuperator is simulated with three heat exchangers. The power consumption of the ASU is obtained considering a specific work of 1049 kJ/kg$_{O2}$, while for the CPU 139.5 kJ/kg is necessary, both according to [26]. The authors implemented an EoS into the model in which the properties of water and steam are calculated using IAPWS_IF97 formulations [41], CO$_2$ is modeled as a real gas using the correlations of NIST REFPROP and the small quantities of O$_2$, N$_2$ and Ar are considered as ideal gases. Regarding the base case, the efficiency of the Net Power cycle is 52.36%, while the Graz cycle efficiency is 52.19%,

considering $CO_2$ purification in both cases. The authors highlighted a slight difference with respect to the results of Scaccabarozzi et al. [10], which is considered by them as a reference in the absence of experimental data: for them this is due to different isentropic and mechanical efficiencies, which lead to a 0.2% points difference, while the remaining 1.2% points are mainly caused by the different EoS models. The authors also conducted a parametric analysis using the IPSEpro-PSOptimize-module in order to optimize the cycle and, consequently, obtain a higher net efficiency. Regarding the Allam cycle, the optimized net efficiency is 52.72%, while the resulting optimized Graz cycle efficiency is 53.5%. In both cases, the $CO_2$ compression and purification and the $O_2$ generation and compression are considered.

Fernandes et al. [42] defined a dynamic model of the integrated ASU—Allam power plant. Simulations were carried out using Aspen Plus v.10, using two different equations of state: the Soave–Redlich–Kwong EoS [43] for the Allam cycle and the Peng-Robinson EoS for the ASU. The high-pressure column and the low-pressure column of the ASU are modeled fixing some parameters and initially calculating the number of stages based on the DSTWU method using the Winn–Underwood–Gilliland method. The ASU power consumption is 0.55 kW/sm3h$_{O2}$, which is equivalent to 1259 kJ/kg$_{O2}$. The combustor is modeled as an RGibbs reactor, while the turbine is modeled considering the three-stage turbine cooling method described by Scaccabarozzi et al. [10]. The recuperator is made up of three sections to avoid temperature cross-over effects. The authors considered two different ASU layouts, comparing the case in which the ASU pumps liquid oxygen instead of compressing it. The net thermal efficiency passes from 59.4% (with an $O_2$ compressor) to 64.3% (with an $O_2$ pump) for a net electric power output of 284 and 305.4 MW, respectively. The authors studied also the effects of the ASU operating parameters on the Allam power cycle and compared the carbon footprint (in g$CO_2$/kWh) of the cycle with natural gas combined cycles.

Scaccabarozzi et al. [44] performed the thermodynamic optimization and part-load analysis of the natural gas-fired NET Power cycle. The optimization has been carried out considering the maximum net electric efficiency as the objective function and several nonlinear and bound constraints. The cycle optimization problem has been tackled with the black-box approach, while the thermodynamic model of the Allam cycle has been developed in Aspen Plus, as yet described by the same authors in [10]. The cycle was optimized using the PSG-COM black-box optimization algorithm [45], resulting in a net electric efficiency of 55.35%, slightly higher than in the previous authors' paper [10].

The off-design behavior of the whole system has been modeled with the strong assumption that the ASU can operate at 40% load while maintaining the same specific energy consumption as at full load. The regenerator has been divided into nine temperature zones, while the off-design curves of the expander have been simplified with the assumption that the non-dimensional mass flow rate remains constant. For a fixed fuel input, the cycle has two independent control variables which are the turbine outlet pressure and the Variable Inlet Guide Vanes (VIGV) angle. Results of the part-load analysis highlighted that in the range of load between 100% and 40% the net electric efficiency decreases with the thermal input decrease to a value between 86% and 83% of the full load efficiency, depending on the TOT level. The efficiency decreasing results are lower with respect to a standard combined cycle efficiency.

Zaryab et al. [46] continued the work started in [44] on the part-load control strategies. The turbine outlet temperature is limited to 725 °C, following the developers' indications shown in [8]. The main improvements to the model are related to the presence of off-design performance maps of compressors, pumps and turbines. The authors tested several control strategies at various part-load operations ranging from 90% down to 20%. As in the previous article, Aspen Plus is the commercial software, that has been chosen for the simulations, with the same principles described in the previous one: the Peng-Robinson EoS has been used, while the cooled turbine has been modeled with the continuous expansion model shown in [10]. The authors investigated four different part-load control strategies:

VC (using variable inlet guide vanes and diffuser guide vanes), HVC (using both minimum cycle pressure variations and the adjustment shown in VC), PHVC (considering also partial admission) and PVC (using variable inlet guide vanes and diffuser guide vanes control mode with partial admission). Results of the simulations showed that between 90% and 60% load, the best control strategy is HVC, while PHVC is the most efficient at lower load. The results highlighted also that the Allam cycle presents a smaller decay of efficiency at part loads when compared with conventional combined cycles when the ASU is designed to maintain a good specific energy consumption at part loads.

### 2.2. Coal-Based Allam Cycle

The peculiarities of the Allam cycle allow us to consider coal as fuel without carbon dioxide emissions, integrating the gasification process within the power cycle.

As written below and reported in Table 1, the coal net efficiency target is equal to 51.44% [5].

In this regard, Luo et al. [47] carried out an exergy-based investigation of an Allam Cycle in the case of the use of coal as fuel. The power cycle has been modeled using the Ebsilon Professional software, considering the real gas properties through the libraries embedded in the software, when necessary. The ASU has been modeled as a black box, with a specific power demand. To maintain the temperature within the desired limits (e.g., TIT < 1150 °C), two controllers are adopted in the simulation. The used methods simplified the continuous expansion model (El-Masri's model), while the recuperative heat exchanger is modeled using a series of heat exchangers. The resulting net efficiency is equal to 41.6% when the turbine inlet temperature is 1150 °C and the turbine pressure ratio is 10, while the exergetic efficiency is 40.5%. The authors highlighted that less than 4% of the fuel exergy is lost in the environment, while 56% is destroyed within the components.

Xin et al. [48] developed a process-splitting analytical method to study the thermo-dynamic performance of a coal-based Allam cycle. The complex system is split into four simple thermal cycles and equivalent heat-to-thermal processes, in order to separate and evaluate the contribution of each section to the overall performance. The simulations were carried out using Aspen Plus. The coal gasification is modeled using the Aspen block Dryer for the dryer, while Rstoic and RGibbs are used for the gasifier. The blocks HeatX, compr and pump were used for the steam generator and steam Rankine cycle. Regarding the Allam cycle, the used blocks are RGibbs (combustor), compr (turbine and compressor models), Valve, Mix, Heater. The recuperator is simulated using the MHeatX block, while the ASU is modeled through compr, Heater, MHeatX, Valve and Sep blocks. Given a raw coal feedstock of 2051.9 MW on an HHV basis, the net efficiency of the overall system is 38.8% on an HHV basis, considering that the efficiencies of the closed $sCO_2$ system and of the steam Rankine cycle are, respectively, 52.68% and 36.6%. The net efficiency of the optimized coal-based cycle is 42.68%.

Zhao et al. [49] carried out a parametric study on the thermodynamic performance of an Allam cycle power plant coupled with a coal gasification process. The simulations are conducted in Aspen plus, using the Peng-Robinson EoS. The water/steam properties have been calculated using the STEAMNBS property method. The recuperator is split into two sections, the combustor is simulated using the RGibbs block. The turbine cooling model is based on the El-Masri continuous expansion model, while the compression unit is simulated through the compr block embedded in Aspen Plus. Regarding the specific power consumption of the other components, for the coal milling and handling and slag handling this is assumed equal to 15 kW h/$t_{coal}$, while for the ASU is 245 kWh/$t_{O2}$. The resulting performance of the base case is a net efficiency of 38.21% for a net power output of 534.89 MW. Results of a parametric study allowed us to increase the performance, up to 38.87%, raising the turbine inlet temperature to 1200 °C and lowering the turbine outlet pressure to 30 bar.

## 2.3. Model Approaches and Results Comparison

Table 2 summarizes the main characteristics of the modeling approaches for the above-mentioned articles: the used software and the choice in terms of the equation of state or correction factors to consider the thermodynamic properties of carbon dioxide in supercritical conditions, beyond the other main embedded sub-models. In cases not explicitly specified, the table refers to steady-state thermodynamic models used to identify the design conditions. A large part of the authors used commercial software.

**Table 2.** Main characteristics of numerical analysis, natural gas case.

| Numerical Analysis | Software | Equation of State/Corrections for sCO$_2$ Properties | Other Main Characteristics | Ref. |
|---|---|---|---|---|
| Thermodynamic analysis | Aspen HYSYS | Lee-Kesler-Plocker | Combustion process: specific heat calculated using the NIST database coupled with Shomate equation | [9] |
| Thermodynamic analysis and cycle optimization | Aspen Plus v8.4 | Peng-Robinson | Regenerator modeled as two multi-flow heat exchangers<br>Turbine model: Modified El-Masri model<br>ASU specific electric consumption at 100 bar: 1365 kJ/kg$_{O2}$. | [10] |
| Exergoeconomic analysis | EBSILON Professional 13 | Peng-Robinson | ASU and recuperator modeled as black-box<br>ASU specific electric consumption: 1447 kJ/kg$_{O2}$.<br>Economic analysis: total revenue requirement method | [25] |
| Exergetic analysis | Aspen Plus | Peng-Robinson; Lee-Kesler-Plöcker for CO$_2$ recompression modeling | Chemical exergy model: Szargut<br>ASU, CO$_2$ purification and cooling tower modeled as black-box<br>ASU Specific consumption: 900 kJ/kg$_{O2}$<br>CO$_2$ Purification: 180 kJ/kg$_{CO2}$ | [27] |
| Thermodynamic analysis | Thermoflex 30 | NIST REFPROP | Turbine modeled as seven cooled gas turbines stages.<br>The cooled gas turbine sub-model is based on El-Masri's code (GASCAN).<br>Regenerator modeled using 3 HX arranged in series. | [29] |
| Thermodynamic analysis and optimization | Aspen ONE | NIST REFPROP | ASU: power consumption; 900 kW/(kg/s), Oxygen purity: 91.25%<br>open-loop internal cooling of HT turbines | [32] |
| Thermodynamic analysis and optimization of reheated cycle | Aspen Plus v11 | - | El-Masri's continuous expansion model for the turbine<br>Regenerator modeled as two multi-flow HX in series<br>Combustor simulated with the RGibbs block<br>ASU specific energy consumption: 245 kWh/t$_{O2}$ | [34] |
| Thermodynamic analysis | Engineering Equation Solver | Ideal gas EoS | negligible pressure drops, adiabatic behavior of all components, no turbine cooling | [35,36] |
| Thermodynamic analysis | Engineering Equation Solver | Ideal gas EoS with correction factors | - | [39] |

**Table 2.** *Cont.*

| Numerical Analysis | Software | Equation of State/Corrections for $sCO_2$ Properties | Other Main Characteristics | Ref. |
|---|---|---|---|---|
| Thermodynamic analysis | IPSEpro v7 | Water/steam: IAPWS_IF97 $CO_2$: NIST REFPROP $N_2$, $O_2$, Ar: ideal gas | ASU specific work: 1049 kJ/kg$_{O2}$, CPU specific work: 139.5 kJ/kg | [40] |
| Thermodynamic and carbon footprint analysis | Aspen Plus v10 | Allam cycle: Soave–Redlich–Kwong ASU: Peng-Robinson | ASU number of stages: DSTWU method using the Winn–Underwood–Gilliland method. ASU specific consumption: 1259 kJ/kg$_{O2}$. Combustor: RGibbs reactor Turbine: three-stage turbine cooling method Recuperator: three sections | [42] |
| Part load thermodynamic analysis | Aspen Plus | See [10] | ASU specific energy consumption fixed in the range 40–100% load Regenerator: nine temperature zones Simplified off design curve of the expander: constant non-dimensional mass flow rate | [44] |
| Part load thermodynamic analysis | Aspen Plus | See [10] | off-design performance maps of compressors, pumps and turbine. | [46] |
| Exergetic analysis | Ebsilon Professional | LibHuGas library LibCO$_2$ library for $CO_2$ | ASU and Acid gradd removal modeled as black box Cooled turbine: The used method simplified the El-Masri's model Recuperator: modeled using a series of heat exchangers | [47] |
| Process splitting analytical model | Aspen Plus | n.a. | Combustor: Rgibbs block Compression unit and turbine: compr blocks Recuperator: MHeatX block | [48] |
| Thermodynamic analysis and parametric study | Aspen Plus | $CO_2$: Peng-Robinson Water/steam: STEAMNBS property | Combustor: RGibbs block Compression unit: compr block Turbine: El-Masri's model Recuperator: splitted in two sections Coal consumption: 65.93 kg/s (1400 MW) | [49] |

The real gas properties of carbon dioxide in trans-critical or supercritical conditions are considered using different equations of state or adopting correction factors or thermodynamic properties databases.

In this regard, Zhao et al. [50] conducted a comparison of six equations of state with experimental data, within the typical operating range of $sCO_2$ Brayton cycles. Their analysis concluded that the Span-Wagner EoS [51] exhibited the highest accuracy across the subcritical, supercritical and critical regions, in the temperature range of 300–900 K and the pressure range of 7–20 MPa. Similarly, Rogalev et al. [32] compared two EoS and the NIST REFPROP database against experimental data [52], concluding that the database, which is based on the aforementioned Span-Wagner EoS, presented the minimum average deviation (0.03%) in $CO_2$ specific volume. The other equations of state showed more significant deviations. Wimmer et al. [40] conducted a comparison between their simulation results and those obtained by Scaccabarozzi et al. [10]. Their analysis revealed that a 1.2-point difference in net efficiency could be attributed to variations in the embedded equation of state. They emphasized that different EoS models led to differences in specific enthalpies, particularly at the turbine inlet and outlet.

Manikantachari et al. [53] compared several EoS with respect to the NIST database with the aim of identifying the best EoS to use within the study of the combustion process. Based on their evaluations, the Peng–Robinson Eos better predicts the thermal state of pure $CO_2$, if compared with Soave–Redlich–Kwong (SRK) [43] and Redlich–Kwong, while, over 1000 K, Peng–Robinson and SRK are indistinguishable. At the same time, for $sCO_2$ combustion mixtures, in all the analyzed regimes, the Soave–Redlich–Kwong and Peng–Robinson EoS predict the density by 0.7% and 1.17% with respect to NIST. The authors concluded that the Soave–Redlich–Kwong is the most appropriate EoS for $sCO_2$ mixtures.

In addition to the choice regarding the modeling of the physical properties of carbon dioxide, the differences in performance indexes could be influenced by the differences in the choice of each component model and in the fixed characteristic parameters (e.g., isentropic efficiency of the rotating components, cooling blades models, effectiveness of the HXs, limits on temperatures). For example, the variations in the proposed ASU specific consumption are in a wide range, between 900 and 1447 kJ/kg$_{O2}$, as highlighted in Table 2. Moreover, with respect to the ASU, whether the role of thermal integration is considered or not can result in significant differences in the overall evaluation of the system's performance.

In the absence of any experimental data, any comparison of numerical results has to consider the concurrent effects of the above-mentioned modeling choices.

For these reasons, it is very hard to identify the best modeling approach and to define the best-optimized layout, but it is only possible to state a performance range in which this novel power plant should operate. With these premises, Tables 3 and 4 report both the main parameter constraints and the results of simulations, in the case of adoption of natural gas or coal-derived fuels, respectively.

**Table 3.** Main parameters and results of numerical analysis, natural gas case.

| Ref. | Main Thermodynamic Parameters | Main Performance Parameters |
|---|---|---|
| [9] | Combustor inlet temperatures (K): O$_2$: 89, CH$_4$: 108, CO$_2$: 525 (gaseous rec.), 214 (liquid rec.)<br>TIT (K): 1417 (liquid CO$_2$ rec.); 1456 (gaseous CO$_2$ rec.) | Net electric Power (MW): 262.4 (liquid CO$_2$ rec.); 324.8 (gaseous CO$_2$ rec.)<br>Net electric Efficiency (%): 44.5 (liquid CO$_2$ rec.); 55.1 (gaseous CO$_2$ rec.) |
| [10] | Pressure levels (bar/bar) 30/300 (base), 47.153/283.62 (opt)<br>Turbine PR: 8.835 (base); 6.015 (opt)<br>TIT (°C): 1150 (base), 1123.79 (opt)<br>TOT (°C): 741.2 (base), 783.81 (opt)<br>Regenerator pinch point: 5 °C | Net electric Power (MWe): 419.31 (base), 421.06 (opt)<br>Net electric efficiency: 54.58% ((base), 54.80% (opt) |
| [25] | TOP (bar): 30<br>TOT (°C): 767 | Net Power Output (MW): 298.1<br>Net electric efficiency = 53.94%<br>Exergetic Efficiency = 50.1%<br>LCOE = 122 €/MWh |
| [27] | Pressure level (bar/bar): 30/300<br>TIT (°C) = 1150 | Net Power (MW): 250<br>Net electric efficiency: 53.4% (base), 47.9 (min), 57.2 (max)<br>Exergetic Efficiency = 51.3% (base), 46% (min), 54.9% (max) |
| [29] | TIP [bar]: 292 (base), 303(opt)<br>TIT [°C]: 1158 (base), 1194 (opt)<br>TOP [bar]: 31 (base), 30 (opt)<br>Turbine pressure levels: 292/31 bar<br>TIT: 1158 °C (base), 1200 °C (opt)<br>TOT: 706 °C | Net electric efficiency [%]: 49% (base), 50.4 (opt)<br>Net Power Output [MW}: 281 (base), 301 (opt)<br>ASU penalty (%LHV): 10.64 (base), 10.66 (opt) |
| [32] | TIT (°C): 1083 (opt)<br>TIP (bar): 300 | Cycle net efficiency: 56.5% (opt)<br>Total specific investment cost (with CCS): $1307.5/kW |
| [34] | Combustor1 Outlet Temperature (°C): 1150<br>Combustor2 Outlet Temperature (°C): 1200<br>TIP (bar): 300 (turbine1), 33 (turbine2)<br>TOP (bar): 34 (base), 31.9 (opt) (turbine1), 3 (base), 2.3 (opt) (turbine2) | Net electrical power (MWe): 903.3 (base), 904.6 (opt)<br>Net electric efficiency = 48.92 (base), 49.32 (opt)<br>Exergetic efficiency = 40.5% |

**Table 3.** *Cont.*

| Ref. | Main Thermodynamic Parameters | Main Performance Parameters |
|---|---|---|
| [35,36] | Turbine inlet temperature(K): 1500 (opt)<br>Turbine inlet pressure (bar): 305.5 (opt)<br>Turbine outlet pressure (bar): 28.1 (opt) | Net cycle efficiency: 54.4% (base), 59.7% (opt) |
| [39] | Turbine inlet temperature(K): 1431<br>Turbine inlet pressure (bar): 300 (base), 358 (opt)<br>Turbine outlet pressure (bar): 30 (base), 28.6 (opt) | Net cycle efficiency: 54.4% (base), 58.2% (opt) |
| [40] | Combustor outlet temperature (°C): 1150<br>Turbine pressure levels (bar/bar): 300/34 | Net cycle efficiency: 52.36% (base), 52.72% (opt)<br>Net cycle efficiency ($O_2$ purity of 97%): 52.21% (base), 52.19% (opt) |
| [42] | Condenser Temperature (°C): −176 (HPC) −192.8 (LPC) | Net Thermal efficiency: 59.4% ($O_2$ compressor), 64.3% ($O_2$ pump)<br>Net electric power (MW): of 284 ($O_2$ compressor) 305.4 net ($O_2$ pump) |
| [44] | Turbine pressure levels (bar/bar): 288.69/47.02<br>Combustor inlet temperature (°C): 1127.7<br>Turbine outlet temperature (°C): 782.7 | Net Electric Power (MWe): 425.26<br>Net Electric Efficiency: 55.35% |
| [46] | TOT (°C) $\leq$ 725 | Net electrical efficiency: 41.5% at 15% load (PHVC) |

**Table 4.** Main parameters and results of numerical analysis, coal-derived fuel case.

| Ref. | Main Thermodynamic Parameters | Main Performance Parameters |
|---|---|---|
| [47] | TIT [°C]: 1150<br>Turbine PR: 10 | Net efficiency: 41.6%<br>Exergetic efficiency: 40.5% |
| [48] | TIT (°C): 1150<br>TIP (bar): 300 | Net efficiency (on HHV basis): 38.8%<br>Net efficiency (opt): 42.68% |
| [49] | TIT (°C): 1150 (base), 1200 °C (opt) | Net efficiency: 38.21% (base), 38.87% (opt) |

Regarding the natural gas case, the target of 58.9% described by the developers and shown in Table 1 and in [5] is not reached in a great part of the simulations. In all the cases, the net electrical efficiency is close to 50% or greater, within a range between 59% and 49%. The optimization of thermodynamic parameters proposed by several authors leads to a slight increase in the performance parameters.

The authors of the reviewed papers agree in affirming that the Allam cycle is one of the most interesting power cycles when natural gas or syngas (from coal or biomass) have to be used when compared with combined cycles with CCS.

## 3. Modifications and Integration to the Allam Cycle

For the aforementioned motivations, part of the researchers' interest has been addressed in the study and definition of both modifications to the Allam cycle and integration of this with other systems. In some cases, the authors proposed also a modification to the cycle name.

Rogalev et al. [54] directed their attention toward the examination of low potential heat recovery, along with suggesting certain modifications to the Allam cycle. The simulations were conducted using AspenONE software. The Peng-Robinson EoS is used to consider the thermo-physical properties of the working fluid. The hydraulic losses in each element's connections were assumed to be zero, while the combustion was considered stoichiometric. The vane/blade cooling effectiveness was determined through thermodynamic analysis, while the internal cooling efficiency was set to 0.7 and the geometrical parameters were obtained using a 1D calculation. The compressed air and the oxygen from the ASU were considered as two heat sources since the first has a maximum thermal power of 29.4 MW while the oxygen at 190 °C has a thermal power of 3.6 MW. A secondary utilization of the compressed air used for oxygen production can lead to an improvement of 3.5% of the net efficiency, addressing this to the regenerative heat exchanger. The simulation

results indicated that a 0.2% increase in efficiency corresponds to a 4.5% rise in the specific investment cost.

Fernandes et al. [55] introduced a multivariable model of predictive control to control and optimization of the Allam cycle: the Dynamic Matrix Control (DMC). The authors used the AspenTech DMC software v11 package, basing the regulatory controlled design on their previous dynamic study on the integrated ASU-Allam cycle, in which the steady-state model was implemented in Aspen Plus and, then, the dynamic model was built in Aspen Dynamics v11 [56]. The application of DMC to the power plant improved the carbon dioxide flow rate, keeping the purity at 97% for the Enhanced oil recovery (EOR) case and allowing the medical purity grade.

Xie et al. [57] proposed the integration of the Allam cycle with a cold energy storage system (CES). The focus of their research was on a techno-economic analysis with a parametric sensitivity analysis. The model was built using gPROMS Process Builder. The cooling turbine model was determined following the modifications proposed by Scaccabarozzi et al. [10] to the El-Masri continuous model. The heat exchanger model was borrowed from Scaccabarozzi et al. [10]. The proposed model was validated against the literature, resulting in a net electric efficiency of 54.55% for a net power output of 419.08 MW. The integration of the Allam cycle with the CES leads to an increase in the net electrical efficiency in the peak-period: 57.80% with respect to 54.55%, while in the valley period, the efficiency is lower (38.81% against 46.98%). More in general, results showed that the CES-Allam system is feasible for load flexible operation in a wider range of power (28.46–105.97%) than that of the Allam cycle (40–100%). The results of the simulation highlighted that the CES-Allam system can present better economic performance with respect to the Allam cycle.

Candelaresi et al. [58] proposed an integrated system for the cogeneration of electricity and the production of substitute natural gas (SNG) from lignocellulosic biomass, water and renewable electricity. This plant, which can serve as energy storage, is based on a modified Allam cycle in which biomass syngas is used instead of natural gas and electrolytic oxygen is used instead of oxygen obtained by the ASU. The aim is to couple a power unit based on the Allam cycle with a water electrolyzer, a biomass gasifier and a methanation section. Simulations have been carried out using Aspen Plus and the chosen EoS is the Peng-Robinson one. The overall efficiency of the proposed system is about 68%, producing 33 MW of net electrical power and 171 MW of SNG (89.2% $CH_4$ and 8.8% $H_2$) chemical power with a thermal power input of 222 MW renewable electricity and 78.6 MW biomass.

Li et al. [59] proposed a dual-pressure Allam cycle integrated with the regasification of liquified natural gas. The cold energy of the LNG is used in the condenser, reducing the heat transfer temperature difference and contributing to enhancing the system performance. The exergy destruction in the condensation process is reduced thanks to the dual-fuel configuration. The model is based on the MATLAB software. The turbine cooling model is taken from Scaccabarozzi et al. [10]. The regenerator has been modeled considering the segmentation method and dividing it into many small sections along the low direction. The ASU was simulated as a black-box and the specific energy consumption is assumed to be 1391 kJ/kg$_{O_2}$. Regarding the classical Allam cycle, the results of the proposed model are coherent with the literature: a net electrical efficiency of 53.06% for a net power output of 407.66 MW. The design performance of the dual-pressure Allam cycle is a net power output of 65.31 MW and a refrigeration capacity of 19.76 MW. The performance indexes of the cogeneration system reported an exergetic efficiency equal to 51.62% for an electricity efficiency of 70.22%. After a parametric analysis and optimization, the optimized dual-pressure Allam cycle presented an electric efficiency of 70.56% and an exergetic efficiency of 51.88%. The specific work was 68.75% higher than the classical case.

Zhu et al. [60] proposed a modified Allam cycle without a compressor, named Allam-Z cycle. All the working media are pumped to high pressure by pumps instead of compressors, while the cold energy of both liquid oxygen and LNG is used for degrading the cooling water for $CO_2$ liquefaction. A set of regenerative heat exchangers are introduced for turbine exhaust recovery. The thermodynamic model has been implemented in MATLAB

and the properties of pure and mixture $CO_2$ and $H_2O$ have been calculated using the REFPROP database (v.8). The power consumption for oxygen production by ASU is set to 0.42 kWh/kg$_{O2}$. The results of this study showed that the output power efficiency and the equivalent net efficiency are 2.15% and 2.96% higher than those of the Allam cycle under the same conditions, respectively: the equivalent net efficiency is 48.05% with respect to the value of 45.09% in both cases, considering a TIT of 900 °C.

Shamsi et al. [61] proposed a new process to produce syngas from the PEM electrolyzer and Allam cycle. The process is made of four units: a water electrolyzer unit, an Allam power cycle, an Organic Rankine Cycle (ORC), and a water/ammonia power cycle. The hydrogen is produced by the water electrolyzer, while the required carbon dioxide for the syngas is obtained from the combustion of LNG in the presence of the oxygen obtained by the water electrolyzer unit, within the Allam cycle. Aspen HYSYS has been used for simulations, considering Peng-Robinson's EoS. Results of thermodynamic simulations showed that the overall efficiency can reach 60.44%, while exergetic efficiency is 63.22%.

Mitchell et al. [62] defined a thermodynamic model of the Allam cycle, proposing novel models of operation to improve plant operational flexibility with the use of liquid oxygen storage, in order to decouple oxygen and electricity production. The Allam Cycle was modeled with the gPROMS Process Building, using the Peng Robinson EoS. Regarding the turbine modeling, the authors used the method proposed by Scaccabarozzi et al. [10,44]. The heat exchangers were discretized into a series of 50 ideal heat exchangers. The authors also investigated the impact of Allam cycle-based plants and liquid oxygen storage on system costs, through the adoption of a purpose-built Unit Commitment and Economic Dispatch model, focusing on the case of Great Britain's electricity system. Results of their simulations found a net cycle efficiency of 58%, while the adoption of novel modes of operation of the cycle and its ASU allowed to decouple oxygen production and electricity production. The Introduction of liquid oxygen (LOX) storage allows for the partial removal of the constraint of the slow dynamics of the ASU and increases the net efficiency by up to 66.10% and the net electricity output by 17.67% when the Allam cycle runs on storage oxygen. Regarding the impact that the Allam cycle power plants with LOX facilitate further, small, reductions in grid $CO_2$ intensities and system costs with respect to the baseline Allam cycle.

Weiland et al. [63] studied an integrated gasification direct-fired sCO$_2$ power cycle based on the Allam cycle, with few modifications. The syngas is compressed and preheated in a cooler and then mixed with $CO_2$ exiting the cycle's HTR, reaching up to 732 °C, passing through another stage of the syngas cooler. Steady state simulations were carried out using Aspen Plus, considering the Peng-Robinson equation of state for the gasification, the ASU, syngas cleaning and CPU sections, and the Lee-Kessler-Plöcker equation of state of the sCO$_2$ power cycle. The capital costs of the plant components have been estimated using the National Energy Technology Laboratory (NETL)'s quality guidelines. The authors compared with reference IGCC plants a baseline case and an improved case. Their results highlighted that the net plant efficiency (on HHV basis) is 37.7% and 40.6 for the baseline and the improved case, respectively. The carbon captured is 97.6% in the first case and 99.4% in the optimized one.

Tian et al. [64] designed the "CAllam" cycle as the combination of coal gasification in supercritical water and the Allam cycle. The authors investigated the cycle and the differences between it and the natural gas Allam cycle through simulations using Aspen Plus. The thermophysical properties have been calculated by combining the Soave–Redlich–Kwong equation of state [43] and the MHV2 mixing model [65]. They concluded that for the CAllam cycle the variation of $CO_2$ recycling ratio has a peak because in that case it not only reduces the temperature of turbine blades but leads to a further improvement of the efficiency. The maximum cycle efficiency is 53.19% for a $CO_2$ recycling ratio of 1.158 and a turbine outlet pressure of 24.3 bar.

Zhou et al. [66] proposed two innovative systems: a coal polygeneration system for ethylene glycol process synthesis and electricity generation integrated with the Allam cycle

(CTEG-AC) and a coal to ethylene glycol process (CTEG) integrated with the Allam cycle and water electrolysis for hydrogen production (CTEG-AEG). The studied layouts have been modeled through Aspen Plus, using the Peng-Robinson EoS for the gaseous components and the IAPWS-95 method for steam/water. The results of the simulations allowed us to compare the two proposed systems with the base case (CTEG). The thermodynamic performance of CTEG-AC is higher than CTEG by 7.11% (46.83% vs. 39.72%), while the CTEG-ACH performance resulted lower (30.65%) and the CTEG-AC process has also the best economic performance.

Byun et al. [67] presented a conceptual process integration between the Haber-Bosch (HB) process with the Allam power cycle. The aim is to reduce the gaseous $CO_2$ emissions associated with traditional ammonia production. The integrated process is studied both in the case of grid-connected and off-grid applications. The integrated process can be divided into the following sections: $sCO_2$ cycle, ASU, steam methane reformer (SMR), HB process, and Pressure swing adsorption (PSA), all modeled using Aspen Plus v11. Regarding the Allam cycle, the authors followed the modeling approach proposed by Mitchell et al. [62]. The authors carried out a termo-economic analysis, obtaining results that the $CO_2$ emission reduction is 68% and 96%, for on-grid and off-grid cases, respectively, when compared to the conventional HB process. From an economic perspective, the study ensures that the process remains economically competitive.

Cha et al. [68] performed a thermodynamic and exergoeconomic analysis of an integrated system, which combines the Allam cycle with the liquified natural gas regasification process. The authors conducted a parametric study and a multi-objective optimization to maximize the exergy efficiency and minimize the total product unit cost. The cycle simulations were carried out using Aspen Plus, while the exergetic, exergoeconomic analysis and the optimization were conducted with MATLAB R2019b (using NSGA-II), which was linked to Aspen Plus v11. The combustor has been modeled based on the theory of Gibbs free energy, while the cooled turbine model was based on El-Masri's continuous expansion model and the regenerator consists of three multi-flow heat exchangers. The chosen EoS was the Peng-Robinson one. Results of simulations highlighted that the Allam-LNG cycle presents a net electrical efficiency of 65.7%, much higher with respect to the base cycle.

Results showed also that there exists a conflicting relation between exergetic efficiency and the cost: the highest efficiency (50.31%) and the lowest cost (16.654 $/GJ) have been reached with different cycle variables.

In Table 5, a summary of the reviewed literature has been listed.

**Table 5.** Integrated energy system based on Allam Cycle.

| Layout Specification | Software | EoS | Main Characteristics and Results | Ref. |
|---|---|---|---|---|
| low potential heat recovery Allam Cycle | AspenONE | Peng-Robinson | Compressed air and oxygen from ASU are considered as heat sources A secondary utilization leads to an improvement of net efficiency of 3.5% | [54] |
| DMC controlled Allam—ASU | Aspen Dynamics v11, Aspentech DMC v11 | See [42] | The application of DMC to the power plant improved the carbon dioxide flow rate, keeping the purity at 97% for the EOR case and allowing the medical purity grade. | [55] |
| CES-Allam | gPROMS Process Builder | n.a. | Increase in the net electric efficiency from 54.55% to 57.80% in peak period Decrease in net efficiency from 46.98% to 38.81% in valley period The CES-Allam system seems to be more flexible, operating in a wide load range (28.46–105–97%) | [57] |

**Table 5.** *Cont.*

| Layout Specification | Software | EoS | Main Characteristics and Results | Ref. |
|---|---|---|---|---|
| Allam Cycle + SNG storage | Aspen Plus | Peng-Robinson | The overall efficiency is about 68%, producing 33 MW of net electrical power and 171 MW of SNG (89.2% $CH_4$ and 8.8% $H_2$) chemical power with a thermal power in input of 222 MW renewable electricity and 78.6 MW biomass. | [58] |
| Dual pressure LNG CES-Allam | Aspen Plus | Peng-Robinson, Lee-Kesler-Plöcker equation for $sCO_2$ | The electric efficiency and specific work of the proposed layout are 15.76% and 68.75% higher than the Allam cycle, respectively, while the dual-pressure Allam cycle exergetic efficiency is equal to 51.88%, with an increase of 1.57% compared with the single-pressure case. | [59] |
| Z-Allam | MATLAB | REFPROP database | The results of this study showed that the output power efficiency and the equivalent net efficiency are 2.15% and 2.96% higher than those of the Allam cycle under the same conditions, respectively: the equivalent net efficiency is 48.05% with respect the value of 45.09%, in both cases considering a TIT of 900 °C | [60] |
| PEM-electrolyzer-Allam-ORC-ammonia/water power cycle | Aspen HYSYS; | Peng-Robinson; | Overall net efficiency: 60.44% Exergetic efficiency: 63.22%. | [61] |
| LOX-Allam | gPROMS Process Building | Peng Robinson | Net cycle efficiency: 58% Novel modes of operation of the cycle and its ASU allowed to decouple oxygen production and electricity production. The Introduction of LOX storage allows to partially remove the constraint of the slow dynamics of the ASU and increase the net efficiency by up to 66.10% and the net electricity output by 17.67% when the Allam cycle runs on storage oxygen. | [62] |
| Allam + gasification | Aspen Plus | Gasification, ASSU, CPU and syngas cleaning: Peng-Robinson $sCO_2$ Power cycle: Lee-Kessler-Plöcker | The net plant efficiency (on HHV basis) is 37.7% and 40.6 for the baseline and the improved case, respectively. The carbon captured is 97.6% in the first case and 99.4% in the optimized one. | [63] |
| CAllam Cycle | Aspen Plus | Soave–Redlich–Kwong + MHV2 mixing model | CAllam cycle is the combination of coal gasification in supercritical water and Allam cycle. The maximum cycle efficiency is 53.19% for a $CO_2$ recycling ratio of 1.158 and a turbine outlet pressure of 24.3 bar | [64] |

**Table 5.** *Cont.*

| Layout Specification | Software | EoS | Main Characteristics and Results | Ref. |
|---|---|---|---|---|
| CTEG + Allam cycle | Aspen Plus | Peng-Robinson steam/water: IAPWS-95 method | The thermodynamic performance of CTEG-AC is higher than CTEG by 7.11% (46.83% vs. 39.72%), while the CTEG-ACH performance resulted lower (30.65%) and CTEG-AC process has also the best economic performance. | [66] |
| Allam cycle + (SMR) + HB process + PSA | Aspen Plus v11 | Peng Robinson | $CO_2$ emission reduction is 68% and 96%, for on-grid and off-grid cases, respectively, when compared to the conventional HB process. From an economic perspective, the study ensures that the process remains economically competitive | [67] |
| Allam cycle + LNG regasification | Aspen Plus v11 + MATLAB R2019b | Peng-Robinson | The Allam-LNG cycle presents a net electrical efficiency of 65.7% Results showed also that there exists a conflicting relation between exergetic efficiency and the cost | [68] |

## 4. Simulation of the Combustion Process

The combustion process must be carried out at high pressure, close to 30 MPa in an ambient mainly composed of carbon dioxide in supercritical conditions. There is a lack of experimental data regarding oxy-fuel combustion in high-pressure, supercritical $CO_2$ and only a few studies have discussed this topic.

Regarding the need for numerical studies of the combustion process in Allam cycle-like conditions, the scarcity of experimental data generates several issues in the validation of the kinetic mechanism, which is a fundamental step to any CFD study.

Concerning this point, some authors tried to adapt or, when possible and in the presence of experimental data, define kinetic mechanisms, which can allow the simulation of the oxy-combustion in the presence of supercritical $CO_2$.

Iwai et al. [13] proposed the adoption of the National University of Ireland, Galway (NUIG) $H_2$-CO chemistry as the basis of the kinetics mechanism, based on Ó Conaire et al. [69]. The authors compared the results of their simulations with a limited set of experimental data and they highlighted that this mechanism gave good results.

Abdul-Sater et al. [70] qualitatively studied the combustion process of a scaled 5 MWth combustor, in order to predict the interior flow, heat transfer and combustion, in the case of syngas fuelling. They coupled a 1D model obtained in Aspen Plus and CFD simulations using Ansys Fluent. The authors employed the Davis mechanism, which consists of 38 reactions and 14 species for the oxidation of CO-$H_2$ [71], while the skeletal mechanism proposed by Smoke was used for fuel blends containing methane in case of adoption of the reactor network model. The Eddy Dissipation Concept (EDC) was used for the turbulent-chemistry interactions. Results of 2D and 3D CFD simulations highlighted that there are no significant temperature or pressure variations in the reaction primary zone and that the estimated CO levels are greater than 100 ppm at 0.99 equivalence ratios, while for an equivalence ratio of 0.9, there is a significant reduction.

Manikantachari et al. [72] defined a reduced mechanism. The authors carried out a comparison between the detailed Aramco 2.0 and GRI 3.0 mechanisms, using various van der Waal's types of equations to predict the ignition delay time. Results of their simulations from shock tubes highlighted that Aramco 2.0 is more accurate in simulating s$CO_2$ combustion applications. After this evaluation, the authors identified a 23-species gas phase mechanism derived from the Aramco 2.0 mechanism as the more appropriate.

Harman-Thomas et al. [73,74] developed a chemical kinetic mechanism for combustion in supercritical carbon dioxide, focusing on the most important fuels for the Allam-Fetvedt cycle (e.g., methane, hydrogen and syngas). They analyzed the available datasets in terms of ignition delay time in any dilution of carbon dioxide for methane, hydrogen or syngas and used four previously published mechanisms: the Aramco 2.0 (493 species and 2716 reactions) [75–78], the DTU mechanism (102 species and 894 reactions) [79,80], the GRI 3.0 (53 species and 325 reactions) [81] and the USC II (111 species and 784 reactions) [82]. The authors used ANSYS Chemkin-Pro 2019 R3 to perform their study in various pressures ranging from sub-atmospheric to over 250 atm, for various $CO_2$ dilutions and equivalence ratios. The results of their study proved the importance of the development of a mechanism specific to oxy-fuel combustion in direct-fired $sCO_2$ power cycles, focusing also on the role of $CH_3O_2$ chemistry in high-pressure methane combustion. The authors declared that quantitative analysis has proven a superior ability to model ignition delay time against existing chemical kinetic mechanisms.

Harman-Thomas et al. [83] measured also the ignition delay time (IDT) of syngas from coal or biomass gasification using a high-pressure shocking tube in pressure and temperature levels typical of the Allam-Fetvedt cycle (20–40 bar and 1100–1300 K). The authors compared their data against the predictions of two different kinetic models (AramcoMech 2.0 and University of Sheffield $sCO_2$ 2.0 Mech [73]).

## 5. Conclusions

Despite the Allam cycle having been recently developed and the absence of any experimental data for the entire energy system, the growing interest of researchers allowed us to confirm the potentialities and highlight the issues.

This review emphasizes the importance of a correct simulation of the thermo-physical properties of the working fluid, with a specific focus on the weight that the choice of the equation of state has on the final simulation results. At the same time, the concurrent effects of each parameter for each component make it impossible to identify the best numerical model approach, because of the lack of experimental data.

With these assumptions, the thermodynamic or thermo-exergetic numerical studies showed that the electric net efficiency of the Allam cycle results higher than the other power system with CCS, even if lower with respect to the values reported by the cycle developers. Some studies focused their attention also on the economic aspects, highlighting the feasibility of this choice.

The opportunities related to the use of coal or biomass-derived syngas as fuel have been described in various studies, as well as the possibility of integration of the Allam cycle in more complex energy systems or with other processes.

In particular, the Allam cycle seems to be widely integrated with other systems, mainly when the integration allows a better use of the waste heat. In this regard, coupling the Allam cycle with LNG regasification seems to lead to very interesting results in terms of performance indexes. Also, the integration with biomass gasification or chemical processes, e.g., ammonia production, seems to give good results.

Regarding the numerical simulations of the combustion process, the main issue is actually related to the choice of the kinetic mechanism, due to the lack of experimental data in Allam-like conditions. Some authors tried to identify novel reduced kinetic mechanisms, exploiting the few available data.

**Conflicts of Interest:** The authors declare no conflict of interest.

**Abbreviations**

| | |
|---|---|
| ASU | Air Separation Unit |
| CCPP | Combined Cycle Power Plant |
| CCS | Carbon Capture and Storage |
| CES | Cold Energy Storage |
| CPU | Compression and Purification Unit |
| CTEG | Coal to Ethylene Glycol process |
| EoS | Equation of State |
| HB | Haber-Bosch |
| HHV | Higher heating value |
| HX | Heat exchanger |
| IGCC | Integrated Gasification Combined Cycle |
| LHV | Lower Heating Value |
| LOX | Liquid Oxygen |
| LNG | liquified Natural Gas |
| NIST | National Institute of Standards and Technology |
| opt | optimized |
| ORC | Organic Rankine Cycle |
| P | Power |
| PEM | Proton Exchange Membrane |
| ppm | parts per million |
| PR | Pressure Ratio |
| RANS | Reynolds averaged Navier Stokes |
| $sCO_2$ | Supercritical carbon dioxide |
| SNG | Synthetic Natural Gas |
| TIP | Turbine Inlet Pressure |
| TIT | Turbine Inlet Temperature |
| TOP | Turbine Outlet Pressure |
| TOT | Turbine Outlet Temperature |
| *Subscripts* | |
| El | Electrical |

**References**

1. Xu, J.; Liu, C.; Sun, E.; Xie, J.; Li, M.; Yang, Y.; Liu, J. Perspective of S−$CO_2$ power cycles. *Energy* **2019**, *186*, 115831. [CrossRef]
2. Ahn, Y.; Bae, S.J.; Kim, M.; Cho, S.K.; Baik, S.; Lee, J.I.; Cha, J.E. Review of supercritical $CO_2$ power cycle technology and current status of research and development. *Nucl. Eng. Technol.* **2015**, *47*, 647–661. [CrossRef]
3. Crespi, F.; Gavagnin, G.; Sanchez, D.; Martinez, G.S. Supercritical carbon dioxide cycles for power generation: A review. *Appl. Energy* **2017**, *195*, 152–183. [CrossRef]
4. Allam, R.J.; Palmer, M.R.; Brown, G.W., Jr.; Fetvedt, J.; Freed, D.; Nomoto, H.; Okita, N.; Jones, C., Jr. High Efficiency and low cost of electricity generation from fossil fuels while eliminating atmospheric emissions including carbon dioxide. *Energy Procedia* **2013**, *37*, 1135–1149. [CrossRef]
5. Allam, R.J.; Fetvedt, J.E.; Forrest, B.A.; Freed, D.A. The Oxy-Fuel, Supercritical $CO_2$ Allam Cycle: New Cycle Developments to Produce Even Lower-Cost Electricity from Fossil Fuels Without Atmospheric Emissions. In Proceedings of the ASME Turbo Expo 2014: Turbine Technical Conference and Exposition, Dusseldorf, Germany, 16–20 June 2014. [CrossRef]
6. Allam, R.J.; Palmer, M.; Brown, G.W. System and Method for High Efficiency Power Generation Using a Carbon Dioxide Circulating Working Fluid. U.S. Patent, 8,596,075 B2, 3 December 2013.
7. Allam, R.J.; White, V.; Miller, E.J. Purification of Carbon Dioxide. U.S. Patent 8,580,206 B2, 12 November 2013.
8. Allam, R.; Martin, S.; Forrest, B.; Fetvedt, J.; Lu, X.; Freed, D.; Brown, G.W., Jr.; Sasaki, T.; Itoh, M.; Manning, J. Demonstration of the Allam Cycle: An update on the development status of a high efficiency supercritical carbon dioxide power process employing full carbon capture. *Energy Procedia* **2017**, *114*, 5948–5966. [CrossRef]
9. Chowdhury, A.; Bugarin, L.; Badhan, A.; Choudhuri, A.; Love, N. Thermodynamic analysis of a directly heated oxyfuelsupercritical power system. *Appl. Energy* **2016**, *179*, 261–271. [CrossRef]
10. Scaccabarozzi, R.; Gatti, M.; Martelli, E. Thermodynamic Analysis and Numerical Optimization of the NET Power Oxy-Combustion Cycle. *Appl. Energy* **2016**, *178*, 505–526. [CrossRef]
11. NET Power Website. First Utility Scale Project. Available online: https://netpower.com/first-utility-scale-project/ (accessed on 25 September 2023).

12. Nomoto, H.; Itoh, M.; Brown, W.; Fetvedt, J.; Sato, I. Cycle and Turbine Development for the Supercritical Carbon Dioxide Allam Cycle. In Proceedings of the International Conference on Power Engineering, Riga, Latvia, 11–13 May 2015.

13. Iwai, Y.; Itoh, M.; Morisawa, Y.; Suzuki, S.; Cusano, D.; Harris, M. Development Approach to the Combustor of Gas Turbine for Oxy-fuel, Supercritical $CO_2$ Cycle. In Proceedings of the ASME Turbo Expo 2015: Turbine Technical Conference and Exposition, Volume 9: Oil and Gas Applications; Supercritical $CO_2$ Power Cycles, Wind Energy, Montreal, QC, Canada, 15–19 June 2015. ASME GT2015-43160.

14. Suzuki, S.; Iwai, Y.; Itoh, M.; Morisawa, Y.; Jain, P.; Kobayashi, Y. High Pressure Combustion Test of Gas Turbine Combustor for 50MWth Supercritical $CO_2$ Demonstration Power Plant on Allam Cycle. In Proceedings of the International Gas Turbine Congress 2019, Tokyo, Japan, 17–22 November 2019.

15. NET Power Website. Second Quarter 2023 Results Report. Available online: https://netpower.com/press-releases/net-power-reports-second-quarter-2023-results-and-provides-business-update/ (accessed on 25 September 2023).

16. Moore, J.J.; Neveu, J.; Bensmiller, J.; Replogle, C.; Lin, J.; Fetvedt, J.; Cormier, I.; Kapat, J.; Fernandez, E.; Paniagua, G. Development of a 300 MWe Utility Scale Oxy-Fuel sCO$_2$ Turbine. In Proceedings of the ASME Turbo Expo Paper no. GT2023-103328, Boston, MA, USA, 26–30 June 2023. [CrossRef]

17. Scopus Document Search. Available online: https://www.scopus.com/ (accessed on 11 September 2023).

18. Web of Science Core Collection. Available online: https://www.webofscience.com/ (accessed on 11 September 2023).

19. Chan, W.; Morosuk, T.; Li, X.; Li, H. Allam cycle: Review of research and development. *Energy Convers. Manag.* **2023**, *294*, 117607. [CrossRef]

20. Lee, B.L.; Kesler, M.G. A generalized thermodynamic correlation based on three-parameter corresponding states. *AIChE J.* **1975**, *21*, 510–527. [CrossRef]

21. Plocker, U.; Knapp, H. Calculation of High-Pressure Vapor-Liquid Equilibria from a Corresponding-States Correlation with Emphasis on Asymmetric Mixtures. *Ind. Eng. Chem. Process Des. Dev* **1978**, *17*, 324–332. [CrossRef]

22. Malcolm, C. NIST-JANAF thermochemical tables. *J. Phys. Chem. Ref. Data Mononograph* **1998**, *1*, 1951.

23. El-Masri, M.A. On thermodynamics of gas-turbine cycles: Part 2—A model for expansion in cooled turbines. *J. Eng. Gas Turbines Power* **1986**, *108*, 151–159. [CrossRef]

24. Peng, D.Y.; Robinson, D.B. A New Two-Constant Equation of State. *Ind. Eng. Chem. Fundam.* **1976**, *15*, 59–64. [CrossRef]

25. Gonzalo, R.H.; Petrakopoulou, F. Exergoeconomic Analysis of the Allam Cycle. *Energy Fuels* **2019**, *33*, 7561–7568. [CrossRef]

26. IEAGHG. *Oxy-Combustion Turbine Power Plants, World Energy Outlook, 2015/05*; OECED/International Energy Agency: Paris, France, 2016. [CrossRef]

27. Penkum, M.; Tsatsaronis, G. Exergy Analysis of the Allam Cycle. In Proceedings of the 5th International Symposium–Supercritical $CO_2$ Power Cycles, San Antonio, TX, USA, 28–31 March 2016.

28. Chou, V.H.; Kearney, D.; Turner, M.J.; Woods, M.C.; Zoelle, A.; Black, J.B. *Quality Guidelines for Energy System Studies: Process Modeling Design Parameters*; Technical Report, DOE/NETL-341/051314; U.S. Department of Energy: Washington, DC, USA, 2014.

29. Colleoni, L.; Sindoni, A.; Ravelli, S. Comprehensive Thermodynamic Evaluation of the Natural Gas-Fired Allam Cycle at Full Load. *Energies* **2023**, *16*, 2597. [CrossRef]

30. Lemmon, E.W.; Bell, I.H.; Huber, M.L.; McLinden, M.O. *NIST Standard Reference Database 23: Reference Fluid Thermodynamic and Transport Properties-REFPROP, Version 10.0*; National Institute of Standards and Technology, Standard Reference Data Program: Gaithersburg, Germany, 2018. [CrossRef]

31. El-Masri, M.A. GASCAN—An interactive code for thermal analysis of gas turbine systems. *J. Eng. Gas Turbines Power* **1988**, *110*, 201–209. [CrossRef]

32. Rogalev, A.; Grigoriev, E.; Kindra, V.; Rogalev, N. Thermodynamic optimization and equipment development for a high efficient fossil fuel power plant with zero emissions. *J. Clean. Prod.* **2019**, *236*, 117592. [CrossRef]

33. Wilcock, R.C.; Young, J.B.; Horlock, J.H. The effect of turbine blade cooling on the cycle efficiency of gas turbine power cycles. *J. Eng. Gas Turbines Power* **2005**, *127*, 109–120. [CrossRef]

34. Chan, W.; Lei, X.; Chang, F.; Li, H. Thermodynamic analysis and optimization of Allam cycle with a reheating configuration. *Energy Convers. Manag.* **2020**, *224*, 113382. [CrossRef]

35. Haseli, Y. Analytical formulation of the performance of the Allam power cycle. In Proceedings of the 2020 ASME Turbo Expo, ASME Paper: GT2020-15070. Virtual, Online, 21–25 September 2020. [CrossRef]

36. Haseli, Y.; Sifat, N.S. Performance modeling of Allam cycle integrated with a cryogenic air separation process. *Comput. Chem. Eng.* **2021**, *148*, 107263. [CrossRef]

37. Haseli, Y. Approximate relations for optimum turbine operating parameters in Allam cycle. *J. Eng. Gas Turbines Power* **2021**, *143*, 064501. [CrossRef]

38. Haseli, Y. Efficiency maximization of Allam cycle at a given combustion temperature. In Proceedings of the 2021 ASME Turbo Expo, Virtual, Online, 7–11 June 2020. ASME Paper: GT2021-59962. [CrossRef]

39. Haseli, Y.; Naterer, G.F. Optimization of turbine pressures in a net-zero supercritical Allam cycle. *J. Clean. Prod.* **2023**, *400*, 136639. [CrossRef]

40. Wimmer, K.; Sanz, W. Optimization and comparison of the two promising oxy-combustion cycles NET Power cycle and Graz Cycle. *Int. J. Greenh. Gas Control* **2020**, *99*, 103055. [CrossRef]

41. Wagner, W.; Kruse, A. *Properties of Water and Steam*; Springer-Verlag: Berlin/Heidelberg, Germany, 1998.

42. Fernandes, D.; Wang, S.; Xu, Q.; Buss, R.; Chen, D. Process and carbon footprint analyses of the Allam cycle power plant integrated with an air separation unit. *Clean Technol.* **2019**, *1*, 22. [CrossRef]

43. Soave, G. Equilibrium constants from a modified Redlich-Kwong equation of state. *Chem. Eng. Sci.* **1972**, *27*, 1197–1203. [CrossRef]

44. Scaccabarozzi, R.; Gatti, M.; Martelli, E. Thermodynamic Optimization and Part-load Analysis of the NET Power Cycle. *Energy Procedia* **2017**, *114*, 551–560. [CrossRef]

45. Martelli, E.; Amaldi, E. PGS-COM: A hybrid method for constrained non-smooth black-box optimization problems. *Comput. Chem. Eng.* **2014**, *63*, 108–139. [CrossRef]

46. Zaryab, S.A.; Scaccabarozzi, R.; Martelli, E. Advanced part-load control strategies for the Allam cycle. *Appl. Therm. Eng.* **2020**, *168*, 114822. [CrossRef]

47. Luo, J.; Emelogu, O.; Morosuk, T.; Tsatsaronis, G. Exergy-based investigation of a coal-fired allam cycle. *Energy* **2021**, *218*, 119471. [CrossRef]

48. Xin, T.; Xu, C.; Yang, Y.; Kindra, V.; Rogalev, A. A new process splitting analytical method for the coal-based Allam cycle: Thermodynamic assessment and process integration. *Energy* **2023**, *267*, 126634. [CrossRef]

49. Zhao, Y.; Wang, B.; Chi, J.; Xiao, J. Parametric study of a direct-fired supercritical carbon dioxide power cycle coupled to coal gasification process. *Energy Convers. Manag.* **2018**, *156*, 733–745. [CrossRef]

50. Zhao, Q.; Mecheri, M.; Neveux, T.; Privat, R.; Jaubert, J.-N. 2016 Thermodynamic Model Investigation for Supercritical $CO_2$ Brayton Cycle for Coal-Fired Power Plant Application. In Proceedings of the Fifth International Supercritical $CO_2$ Power Cycles Symposium, San Antonio, TX, USA, 29–31 March 2016. Paper No. 93.

51. Span, R.; Wagner, W. A new equation of state for carbon dioxide covering the fluid region from the triple-point temperature to 1100 K at pressures up to 800 MPa. *J. Phys. Chem. Ref. Data* **1996**, *25*, 1509–1558. [CrossRef]

52. Vargaftik, N.B. *Handbook of Thermophysical Properties of Gases and Liquids*; Nauka: Moscow, Russia, 1972; p. 721.

53. Manikantachari, K.R.V.; Martin, S.; Bobren-Diaz, J.O.; Vasu, S. Thermal and Transport Properties for the Simulation of Direct-Fired $sCO_2$ Combustor. *ASME. J. Eng. Gas Turbines Power* **2017**, *139*, 121505. [CrossRef]

54. Rogalev, A.; Rogalev, N.; Kindra, V.; Zlyvko, O.; Vegera, A. A Study of Low-Potential Heat Utilization Methods for Oxy-Fuel Combustion Power Cycles. *Energies* **2021**, *14*, 3364. [CrossRef]

55. Fernandes, D.; Haque, M.E.; Palanki, S.; Rios, S.G.; Chen, D. DMC controller design for an integrated Allam cycle and air separation plant. *Comput. Chem. Eng.* **2020**, *141*, 107019. [CrossRef]

56. Fernandes, D.; Wang, S.; Xu, Q.; Chen, D. Dynamic simulations of the Allam cycle power plant integrated with an air separation unit. *Int. J. Chem. Eng.* **2019**, *2019*, 6035856. [CrossRef]

57. Xie, M.; Chen, L.; Wu, K.; Liu, Z.; Lin, J.; Jiang, C.; Xie, S.; Zhao, Y. A novel peak shaving approach to improving load flexibility of the Allam cycle by integrating cold energy storage. *J. Clean. Prod.* **2023**, *386*, 135769. [CrossRef]

58. Candelaresi, D.; Spazzafumo, G. Production of Substitute Natural Gas Integrated with Allam Cycle for Power Generation. *Energies* **2023**, *16*, 2162. [CrossRef]

59. Li, B.; Wang, S.; Qiao, J.; Wang, B.; Song, L. Thermodynamic analysis and optimization of a dual-pressure Allam cycle integrated with the regasification of liquefied natural gas. *Energy Convers. Manag.* **2021**, *246*, 114660. [CrossRef]

60. Zhu, Z.; Chen, Y.; Wu, J.; Zhang, S.; Zheng, S. A modified Allam cycle without compressors realizing efficient power generation with peak load shifting and $CO_2$ capture. *Energy* **2019**, *174*, 478–487. [CrossRef]

61. Shamsi, M.; Moghaddas, S.; Torabi, O.; Bakhshehshi, S.; Bonyadi, M. Design and analysis of a novel structure for green syngas and power cogeneration based on PEM electrolyzer and Allam cycle. *Int. J. Hydrogen Energy* **2023**, *48*, 29034–29047. [CrossRef]

62. Mitchell, C.; Avagyan, V.; Chalmers, H.; Lucquiaud, M. An initial assessment of the value of Allam Cycle power plants with liquid oxygen storage in future GB electricity system. *Int. J. Greenh. Gas Control* **2019**, *87*, 1–18. [CrossRef]

63. Weiland, N.T.; White, C.W. Techno-economic analysis of an integrated gasification direct-fired supercritical $CO_2$ power cycle. *Fuel* **2018**, *212*, 613–625. [CrossRef]

64. Tian, Y.; Feng, H.; Zhang, Y.; Li, Q.; Liu, D. New insight into Allam cycle combined with coal gasification in supercritical water. *Energy Convers. Manag.* **2023**, *292*, 117432. [CrossRef]

65. Dahl, S.; Fredenslund, A.; Rasmussen, P. The MHV2 Model: A UNIFAC-Based Equation of State Model for Prediction of Gas Solubility and Vapor-Liquof State Model for Prediction of Gas Solubility and Vapor-Liquid Equilibria at Low and High Pressures. *Ind. Eng. Chem. Res.* **1991**, *30*, 1936–1945. [CrossRef]

66. Zhou, Y.; Xu, Z.; Zhang, J.; Xing, J.; Jia, J.; Cui, P. Development and techno-economic evaluation of coal to ethylene glycol process and Allam power cycle and carbon capture and storage and integration process. *Fuel* **2023**, *332*, 126121. [CrossRef]

67. Byun, M.; Lim, D.; Lee, B.; Kim, A.; Lee, I.; Brigljević, B.; Lim, H. Economically feasible decarbonization of the Haber-Bosch process through supercritical $CO_2$ Allam cycle integration. *Appl. Energy* **2022**, *307*, 118183. [CrossRef]

68. Chan, W.; Li, H.; Li, X.; Chang, F.; Wang, L.; Feng, Z. Exergoeconomic analysis and optimization of the Allam cycle with liquefied natural gas cold exergy utilization. *Energy Convers. Manag.* **2021**, *235*, 113972. [CrossRef]

69. Ó'Conaire, M.; Curran, H.J.; Simmie, J.M.; Pitz, W.J.; Westbrook, C.K. A comprehensive modelling study of hydrogen oxidation. *Int. J. Chem. Kinet.* **2004**, *36*, 603–622. [CrossRef]

70. Abdul-Sater, H.; Lenertz, J.; Bonilha, C.; Lu, X.; Fetvedt, J. A CFD simulation of coal syngas oxy-combustion in a high-pressure supercritical $CO_2$ environment. In *Turbo Expo: Power for Land, Sea, and Air*; ASME Paper: GT2017-63821; American Society of Mechanical Engineers: New York, NY, USA, 2017; Volume 50848. [CrossRef]

71. Davis, S.G.; Ameya, V.J.; Hai, W.; Fokion, E. An optimized kinetic model of H$_2$/CO combustion. 1. *Proc. Combust. Inst.* **2005**, *30*, 1283–1292. [CrossRef]

72. Manikantachari, K.R.V.; Vesely, L.; Martin, S.; Bobren-Diaz, J.O.; Vasu, S. Reduced Chemical Kinetic Mechanisms for Oxy/Methane Supercritical CO$_2$ Combustor Simulations. *ASME J. Energy Resour. Technol.* **2018**, *140*, 092202. [CrossRef]

73. Harman-Thomas, J.M.; Pourkashanian, M.; Hughes, K.J. Chemical kinetic mechanism for combustion in supercritical carbon dioxide. In Proceedings of the 4th Eurpean SCO$_2$ Conference Energy Systems, Online, 22–26 March 2021; Volume 255.

74. Harman-Thomas, J.M.; Hughes, K.J.; Pourkashanian, M. The development of a chemical kinetic mechanism for combustion in supercritical carbon dioxide. *Energy* **2022**, *255*, 124490. [CrossRef]

75. Burke, U.; Metcalfe, W.K.; Burke, S.M.; Heufer, K.A.; Dagaut, P.; Curran, H.J. A detailed chemical kinetic modeling, ignition delay time and jet-stirred reactor study of methanol oxidation. *Combust. Flame* **2016**, *165*, 125–136. [CrossRef]

76. Burke, S.M.; Burke, U.; Mc Donagh, R.; Mathieu, O.; Osorio, I.; Keesee, C.; Morones, A.; Petersen, E.L.; Wang, W.; DeVerter, T.A.; et al. An experimental and modeling study of propene oxidation. Part 2: Ignition delay time and flame speed measurements. *Combust. Flame* **2015**, *162*, 296–314. [CrossRef]

77. Burke, S.M.; Metcalfe, O.; Herbinet, F.; Battin-Leclerc, F.M.; Haas, J.; Santner, F.L.; Dryer, H.J.; Curran, H.J. An experimental and modeling study of propene oxidation. Part 1: Speciation measurements in jet-stirred and flow reactors. *Combust. Flame* **2014**, *161*, 2765–2784. [CrossRef]

78. Kéromnès, A.W.K.; Metcalfe, K.A.; Heufer, N.; Donohoe, A.K.; Das, C.-J.; Sung, J.; Herzler, C.; Naumann, P.; Griebel, O.; Mathieu, M.C.; et al. An experimental and detailed chemical kinetic modeling study of hydrogen and syngas mixture oxidation at elevated pressures. *Combust. Flame* **2013**, *160*, 995–1011. [CrossRef]

79. Hashemi, H.; Christensen, J.M.; Glarborg, P. High-pressure pyrolysis and oxidation of DME and DME/CH4. *Combust. Flame* **2019**, *205*, 80–92. [CrossRef]

80. Hashemi, H.; Christensen, J.M.; Gersen, S.; Levinsky, H.; Klippenstein, S.J.; Glarborg, P. High-pressure oxidation of methane. *Combust. Flame* **2016**, *172*, 349–364. [CrossRef]

81. Smith, G.P.; Golden, D.M.; Frenklach, M.; Moriarty, N.W.; Eiteneer, B.; Goldenberg, M.; Bowman, C.T.; Hanson, R.K.; Song, S.; Gardiner, W.C.; et al. GRI Mechanism 3.0. Available online: http://combustion.berkeley.edu/gri-mech/version30/text30.html (accessed on 15 September 2023).

82. Wang, H.; You, X.; Joshi, A.V.; Davis, S.G.; Laskin, A.; Egolfopoulos, F.; Law, C. USC Mech Version II. High-Temperature Combustion Reaction Model of H$_2$/CO/C1-C4 Compounds. 2007. Available online: https://ignis.usc.edu:80/Mechanisms/USC-Mech%20II/USC_Mech%20II.htm (accessed on 25 September 2023).

83. Harman-Thomas, J.M.; Kashif, T.A.; Hughes, K.J.; Pourkashanian, M.; Farooq, A. Experimental and modelling study of syngas combustion in CO$_2$ bath gas. *Fuel* **2023**, *342*, 127865. [CrossRef]